Dalton Transactions

ROYAL SOCIETY OF CHEMISTRY

COMMUNICATION

View Article Online
View Journal | View Issue

Cite this: *Dalton Trans.*, 2022, **51**, 16795

Received 16th August 2022,
Accepted 28th September 2022

DOI: 10.1039/d2dt02680e

rsc.li/dalton

A new supramolecular bonding motif involving NH bonds of ammonium salts and macrocycles derived from platinum corners and butadiynediyl linkers†

Brenna K. Collins, Nattamai Bhuvanesh and John A. Gladysz *

CuI catalyzes reactions of *cis*-$(R_2C(CH_2PPh_2)_2)Pt(C{\equiv}CC{\equiv}CH)_2$ and *cis*-$(R_2C(CH_2PPh_2)_2)PtI_2$ in secondary amine solvents HNR'_2 to give the title adducts $[(R_2C(CH_2PPh_2)_2)Pt(C{\equiv}CC{\equiv}C)]_4{\cdot}(H_2NR'_2{}^+I^-)_n$ (R/R′/*n* = Me/Et/1, Me/$((CH_2CH_2)_2O)_{0.5}$/3, Et/Et/1, Et/$CH_2CH{=}CH_2$/1; 92–42%). Crystal structures of these or closely related species establish folded Pt_4 cores containing ammonium cation guests, with NH/ and NCH/C≡C hydrogen bonding. DOSY NMR experiments show that the host/guest relationship can be maintained in solution.

Supramolecular chemistry features two ubiquitous compositional elements that can come into play both independently and in concert: macrocyclic hosts and hydrogen bonding.[1] Some of the wide range of hydrogen bond donors and acceptors have biological roots[2] or are bio-inspired,[3] and others result from molecular design.[4,5] However, it is very unusual these days for new and effective hydrogen bonding partners to emerge "out of the blue". In this communication, an unexpected new family of hydrogen bond acceptors, four-sided Pt_4C_{16} macrocycles **I** (Scheme 1) that feature platinum corners and butadiynediyl edges, is disclosed.

We and three other groups (Youngs, Bruce, Anderson)[6–9] have reported syntheses of **I** by the route shown in Scheme 1, which involves a *cis* monoplatinum bis(butadiynyl) complex, a *cis* monoplatinum dichloride complex, a CuI catalyst, and a secondary amine cosolvent such as $HNEt_2$. For heretofore obscure reasons, in nearly all cases the ammonium salt byproduct $H_2NEt_2{}^+Cl^-$ has been very difficult to remove, with the solid materials initially isolated best represented as $\mathbf{I}{\cdot}(H_2NEt_2{}^+Cl^-)_n$.[7–9] Other secondary amines as well as tertiary amines gave similar results.

Although we investigated reactions with six different 1,3-diphosphine ligands and numerous workups, analytically pure ammonium-salt-free samples were never obtained.[9] NMR spectra typically showed 1–2 equivalents of the salt, four of which are generated per macrocycle. Nonetheless, by difficultly reproducible procedures, salt-free single crystals could be grown in three cases. Three further crystalline samples, but none that incorporated ammonium salts, were obtained by Bruce.[8] The six X-ray structures showed both planar and folded Pt_4 conformations, as quantified by the angle between the two Pt–Pt–Pt planes that constitute the "hinge leaves" (0° for planar macrocycle). DFT computations suggested these to be very close in energies, separated by a miniscule barrier, and thereby dictated by packing forces.[9]

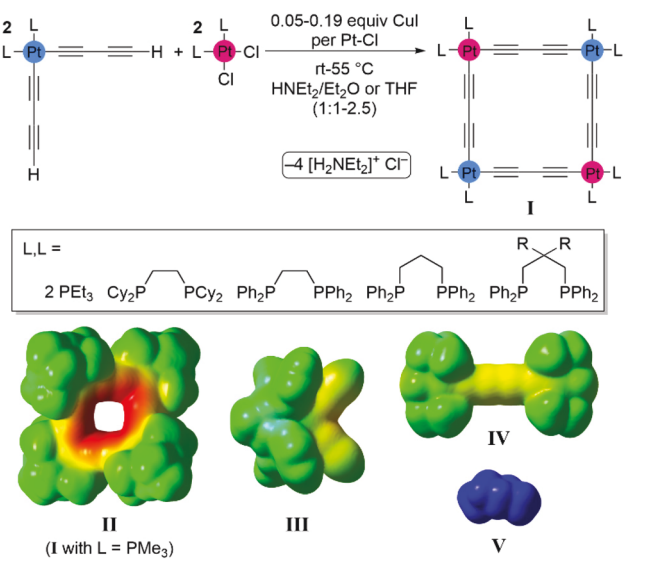

Scheme 1 Prior syntheses of Pt_4C_{16} complexes (**I**; top), and electrostatic potential energy maps for the model compounds $[(Me_3P)_2Pt(C{\equiv}C)_2]_4$ (**II**), *cis*-$(Me_3P)_2Pt((C{\equiv}C)_2H)_2$ (**III**), *trans*,*trans*-$(Me_3P)_2(Me)Pt(C{\equiv}C)_4Pt(Me)(PMe_3)_2$ (**IV**), and $[H_2NEt_2]^+$ (**V**).

Department of Chemistry, Texas A&M University, PO Box 30012, College Station, Texas 77842-3012, USA. E-mail: gladysz@mail.chem.tamu.edu

†Electronic supplementary information (ESI) available: Experimental procedures, spectroscopic and crystallographic data. CCDC 2183176–2183178. For ESI and crystallographic data in CIF or other electronic format see DOI: https://doi.org/10.1039/d2dt02680e

In our previous report[9] we computed electrostatic potential energy maps, as exemplified by **II–IV** in Scheme 1. The first shows a marked negatively charged region associated with the Pt_4C_{16} core. The analogous Pt_5C_{20} or triangular Pt_3C_{12} species exhibit the same charge density pattern, suggesting that this entire series of compounds could be effective hosts for ammonium cations, per the typical electrostatic energy map **V** (Scheme 1). With related *cis*-$L_2Pt(C{\equiv}C)_nH$ species (n = 1, 2), for which various types of π adducts of the C≡C linkages have been characterized,[10] no markedly negative region is apparent (**III**, n = 2). The same holds for complexes with $Pt(C{\equiv}C)_nPt$ linkages (*e.g.*, **IV**). Thus, the high negative charge density is not an embodiment of the Pt_yC_{4y} corners or linkers, but rather a characteristic realized upon generation of the macrocycle.

Accordingly, we sought to physically substantiate specific **I**/ammonium salt bonding interactions. After repeated efforts to obtain X-ray structures of marginal crystals, the dichloride building blocks in Scheme 1 were changed to the corresponding diiodides to match the copper halide catalyst used (CuI). Reactions were set up as summarized in Scheme 2 using two chelating 1,3-diphosphines ($Ph_2PCH_2CR_2CH_2PPh_2$; R = Me, Et) that lead to Pt_4C_{16} macrocycles **1** and **2**, and three secondary amine cosolvents (**a**, $HNEt_2$; **b**, $HN(CH_2CH{=}CH_2)_2$, **c**, morpholine). An analogous reaction was carried out with the tertiary amine NEt_3 (**d**). The Pt_4C_{16}/ammonium iodide adducts **1**·H**a**$^+$I$^-$, **1**·(H**c**$^+$I$^-$)$_3$, **2**·H**a**$^+$I$^-$, **2**·H**b**$^+$I$^-$, and **2**·(H**d**$^+$I$^-$)$_3$ precipitated as yellow solids in 92–42% yields. The NMR properties closely matched those of diethyl- or triethylammonium chloride species isolated earlier.[9] The stoichiometry with respect to the ammonium iodide salts (1–3 equiv.) was established by ^{1}H NMR and microanalyses.

With effort, crystals of solvates of the preceding adducts could be reproducibly obtained. Structural characterization was hampered by rapid partial desolvation upon removal from the mother liquor, solvate leaching into the oils commonly used during data collection, disorder, and other problems.[11] Nonetheless, three structures could be solved, all featuring a single ammonium halide per macrocycle: **1**·H**a**$^+$I$^-$·1.62CH_2Cl_2, **2**·H**b**$^+$I$^-$·3.75$CHCl_3$·2.83C_7H_8, and **1**·H**c**$^+$Cl$^-$. The chloride anion in the last salt is believed to arise from the CH_2Cl_2 solvent, perhaps by reaction with the original iodide anion during the crystallization period.[12]

As shown in Fig. 1, the ammonium cations were strongly associated with the Pt_4C_{16} macrocycles, consistent with expectations from electrostatic effects alone. The macrocycles were moderately to sharply folded, with the hinge planes (Pt1–Pt2–Pt4 and Pt2–Pt3–Pt4) defining angles of 144°, 135°, and 96°, respectively. A representative overall structure is depicted in Fig. 2. The crystal structures of ammonium-salt-free **1** and **2** determined earlier (see above)[9] gave hinge plane/hinge plane angles of 111° and 138–135° (two solvates). Interestingly, **1** opens from 111° to 144° to accommodate the guest in **1**·H**a**$^+$I$^-$·1.62CH_2Cl_2, but "bites down" to 96° in **1**·H**c**$^+$Cl$^-$.

In all three structures, the NH hydrogen atoms (shaded blue) were clearly bonding to the C_4 linkages of the macrocycles. As sketched for the diethylammonium salt **1**·H**a**$^+$I$^-$·1.62CH_2Cl_2 in Fig. 1 (top), the two NH atoms exhibited short NH···$(C{\equiv}C)_{centroid}$ contacts of 2.41 and 2.84 Å. The NH···C_{sp} distances are tabulated in the ESI.† With the diallylammonium salt **2**·H**b**$^+$I$^-$·3.75$CHCl_3$·2.83C_7H_8, only one short NH···$(C{\equiv}C)_{centroid}$ contact was evident (2.70 Å). With the morpholinium salt **1**·H**c**$^+$Cl$^-$, four were found (2.89, 3.10, 2.48, 2.59 Å). These are well within typical distances for NH hydrogen bonds to heteroatoms bearing lone pairs.[13] The corresponding N···$(C{\equiv}C)_{centroid}$ distances, which are more accurately

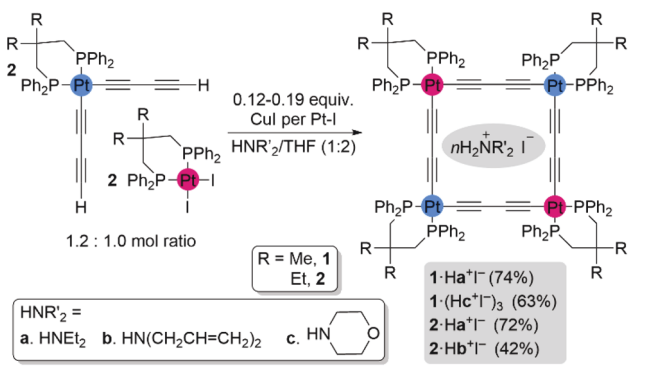

Scheme 2 Syntheses of Pt_4C_{16}/dialkylammonium iodide adducts.

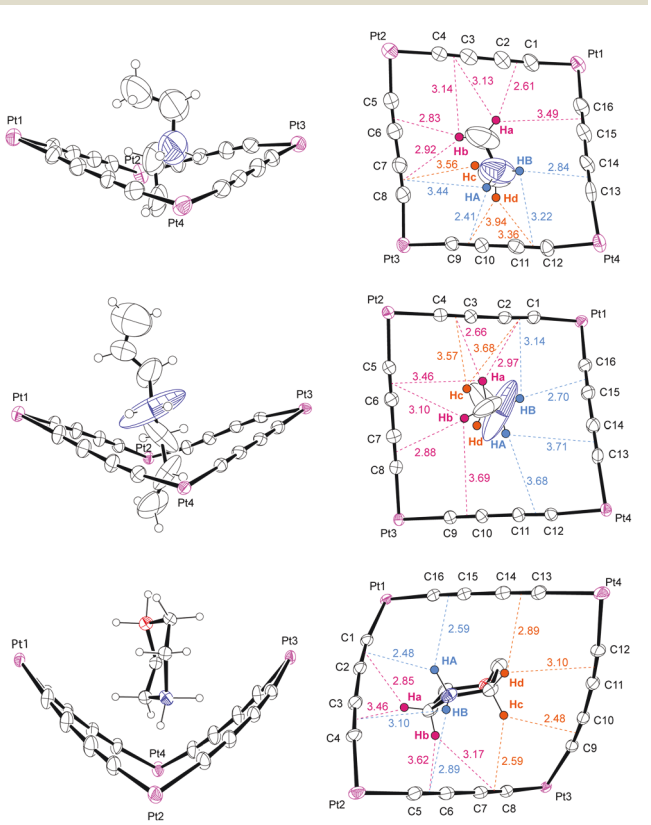

Fig. 1 Structures of the Pt_4C_{16} macrocycles and ammonium cations of **1**·H**a**$^+$I$^-$·1.62CH_2Cl_2 (top), **2**·H**b**$^+$I$^-$·3.75$CHCl_3$·2.83C_7H_8 (middle), and **1**·H**c**$^+$Cl$^-$ (bottom) (thermal ellipsoids at 50% level).

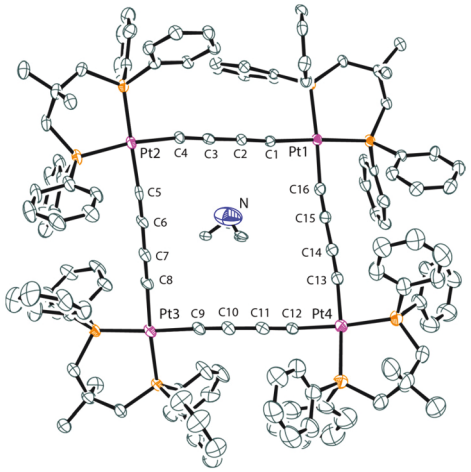

Fig. 2 Structure of $\mathbf{1}\cdot Ha^{+}I^{-}\cdot 1.62CH_2Cl_2$, with the solvent molecules and I^- ion omitted (thermal ellipsoids at 50% probability level except 10% for the carbon atoms of the diethylammonium salt.

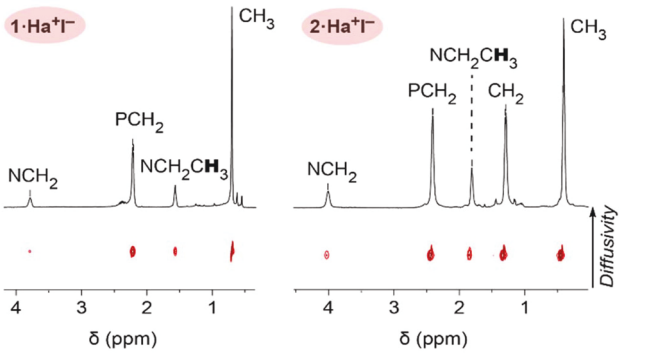

Fig. 3 DOSY ^{1}H NMR plots of $\mathbf{1}\cdot Ha^{+}I^{-}$ and $\mathbf{2}\cdot Ha^{+}I^{-}$ (500 MHz, $CDCl_3$, upfield signals; full spectra are given in the ESI†).

determined, are also given in the ESI† (closest contacts 3.27–3.58 Å).

It is also well established that the NCH hydrogen atoms of ammonium salts can serve as hydrogen bond donors.[14] Similarly close NCH···$(C{\equiv}C)_{centroid}$ and NC···$(C{\equiv}C)_{centroid}$ contacts are evident in the preceding crystal structures (see atoms and distances in red). For example, the shortest NH···$(C{\equiv}C)_{centroid}$ distances in $\mathbf{1}\cdot Ha^{+}I^{-}\cdot 1.62CH_2Cl_2$ are 2.61, 2.83, and 2.92 Å. Comparable distributions are found in the other structures, as tabulated in the ESI.† Importantly, attempts were made to crystallize a variety of related adducts. While only the three structures in Fig. 1 could be solved at a sufficient level, others with chelating diphosphines bearing *p*-C_6H_4X in place of phenyl groups unmistakably gave analogous host/guest adducts.[15]

Next, attention was turned to probing macrocycle/ammonium cation interactions in solution, using the samples isolated in Scheme 2. In all cases, non-overlapping ^{1}H NMR signals were available, facilitating diffusion ordered spectroscopy (DOSY) experiments.[16] The customary magnetic field gradient was applied along the *z* axis, and a series of spectra were recorded in $CDCl_3$. These exhibited the usual decay of signal intensities with increasing gradient strengths, from which the diffusion coefficients in Table S5† were calculated.

DOSY ^{1}H NMR plots of $\mathbf{1}\cdot Ha^{+}I^{-}$ and $\mathbf{2}\cdot Ha^{+}I^{-}$ are depicted in Fig. 3 and S1–S2.† It is easily seen that the diffusion coefficients of the macrocycle and cation are practically identical in both cases, indicating a very high degree of association ($D \times 10^{10}$, $m^2\ s^{-1}$: 3.96–4.05 for seven signals in $\mathbf{1}\cdot Ha^{+}I^{-}$, and 3.75–3.79 for eight signals in $\mathbf{2}\cdot Ha^{+}I^{-}$). Comparable agreement was found in CD_2Cl_2 (Table S5†). The 1 : 1 adduct $\mathbf{2}\cdot Hb^{+}I^{-}$ also showed appreciable correlation (Fig. S5 and Table S5†), although the cation signals gave *D* values *ca.* 15% greater than those of the macrocycle. However, with the 1 : 3 adducts $\mathbf{1}\cdot(Hc^{+}I^{-})_3$ and $\mathbf{2}\cdot(Hd^{+}I^{-})_3$, the cations and macrocycles exhibited markedly different diffusivities (Fig. S3, S4 and Table S5;† 100% greater for the cations). This trend is not surprising, as all crystallized samples feature only a single ammonium cation, suggesting stronger interactions of the macrocycle with the first cation. Thus, additional ammonium cations become progressively more weakly bound, and since rapid exchange would be expected, their diffusivities show less and less correlation to the macrocycle.

Other potential probes of macrocycle/ammonium cation interactions were investigated. Mass spectra of the preceding samples generally showed signals corresponding to ammonium cation adducts ($\mathbf{1}\cdot H_2\mathbf{a}^{2+}$ (85%), $\mathbf{2}\cdot H_2\mathbf{a}^{2+}$ (100%), $\mathbf{2}\cdot H\mathbf{d}^{+}$ (20%), $\mathbf{1}\cdot H_2\mathbf{c}^{+}$ (100%), and $\mathbf{2}\cdot H\mathbf{b}^{+}$ (7%)). Bruce observed similar H_2NEt_2-containing ions with isolated samples of his Pt_4C_{16} adducts (**I**, L_2 = $2PEt_3$, dppe, dppp).[7] Under carefully controlled conditions in solution, the IR ν_{NH} bands of ammonium salts[17] can be effective probes of hydrogen bonding.[18] However, none of the products in Scheme 2 exhibited detectable absorptions under ATR IR conditions (powder film), although ν_{CH} bands were plainly visible.

Others have interrogated the hydrogen bond acceptor abilities of C≡C units.[18,19] It is not unusual in crystal structures of C≡CH species to find C≡CH···$(C{\equiv}C)_{centroid}$ interactions involving neighboring molecules.[19] Two AuC≡CAu adducts have been crystallized as $CHCl_3$ solvates, with $Cl_3CH\cdots(C{\equiv}C)_{centroid}$ distances of 2.42–2.58 Å that were interpreted as CH/π interactions.[20] In a detailed study of $[n\text{-}Oct_3NH]^{+}$ $[B(C_6F_5)_4]^{-}$ in non-polar CCl_4 solutions,[18] 3-hexyne was found to be a weak hydrogen bond acceptor, comparable to cycloalkenes (albeit stronger than methylbenzenes $C_6H_{6-n}Me_n$ (n = 0–6), conjugated dienes and terminal alkynes). In any case, none of these C≡C based acceptors come close to the voracities that characterize the Pt_4C_{16} systems **1** and **2**.

In integrating the preceding data for Pt_4C_{16}/ammonium cation systems, the relative importance of electrostatic and hydrogen bonding interactions is challenging to assess. Furthermore, a reviewer has noted the possible relevancy of cation/π interactions.[21] The electronic structures of close models for the Pt_4C_{16} macrocycles have been characterized by

time-dependent DFT calculations,[9] and provide no obvious origin of the surface charge distribution in **II** (Scheme 1). NICS calculations reveal no "ring current" effects, and there is little evidence for significant electronic interactions between alkynyl ligands in *cis*-$L_2Pt((C{\equiv}C)_nR)_2$ systems.[22] Additional studies with tetraalkylammonium salts could potentially provide some clarification, but obvious guest cations such as $^{+}N(CH_3)_4$ might nonetheless engage in NCH hydrogen bonding.[23]

To sum, since (1) the surface charge distribution in **I** has no counterpart in any monoplatinum or diplatinum model compounds, and (2) strong hydrogen bonding interactions of non-terminal alkynes and ammonium salts have not been previously documented, it seems appropriate to view the Pt_4C_{16}/ammonium cation adducts as new types of macrocycle-based supramolecular assemblies based upon a combination of electrostatic and hydrogen bonding interactions. Macrocycles capable of binding cationic guests have played a foundational role in supramolecular chemistry, and these new systems potentially represent springboards as far-reaching as 18-crown-6/K^+ or 18-crown-6/RNH_3^+. Thus, it appears urgent to further probe the scope of this bonding motif, particularly with respect to the corner elements, the lengths of the $(C{\equiv}C)_n$ segments, and additional types of cations and hydrogen bond donors.

Conflicts of interest

There are no conflicts to declare.

Acknowledgements

The authors thank the US National Science Foundation (CHE-1566601, CHE-1900549) for support, and Prof. T. Lis (University of Wrocław) for helpful discussions.

References

1 J. W. Steed and J. L. Atwood, *Supramolecular Chemistry*, Wiley, New York, 2000, ch. 1.7.4, 5.3.4.7, 6.1.3.
2 N. B. Leontis, J. Stombaugh and E. Westhof, *Nucleic Acids Res.*, 2002, **30**, 3497–3531.
3 (*a*) S.-K. Chang and A. D. Hamilton, *J. Am. Chem. Soc.*, 1988, **110**, 1318–1319; (*b*) A. Tron, M. Rocher, P. J. Thornton, J. H. R. Tucker and N. D. McClenaghan, *Asian J. Org. Chem.*, 2015, **4**, 192–202.
4 L. J. Karas, C.-H. Wu, R. Das and J. I.-C. Wu, *Wiley Interdiscip. Rev.: Comput. Mol. Sci.*, 2020, **10**, e1477, DOI: 10.1002/wcms.1477.
5 D. A. Leigh, C. C. Robertson, A. M. Z. Slawin and P. I. T. Thomson, *J. Am. Chem. Soc.*, 2013, **135**, 9939–9943.
6 S. M. ALQaisi, K. J. Galat, M. Chai, D. G. Ray, P. L. Rinaldi, C. A. Tessier and W. J. Youngs, *J. Am. Chem. Soc.*, 1998, **120**, 12149–12150.
7 M. I. Bruce, K. Costuas, J.-F. Halet, B. C. Hall, P. J. Low, B. K. Nicholson, B. W. Skelton and A. H. White, *J. Chem. Soc., Dalton Trans.*, 2002, 383–398.
8 M. Janka, G. K. Anderson and N. P. Rath, *Organometallics*, 2004, **23**, 4382–4390.
9 B. K. Collins, M. C. Mastry, A. Ehnbom, N. Bhuvanesh, M. B. Hall and J. A. Gladysz, *Chem. – Eur. J.*, 2021, **27**, 10021–10039.
10 (*a*) J. Forniés, E. Lalinde, F. Martínez, M. T. Moreno and A. J. Welch, *J. Organomet. Chem.*, 1993, **455**, 271–281; (*b*) C. J. Adams and P. R. Raithby, *J. Organomet. Chem.*, 1999, **578**, 178–185; (*c*) J. Fernández, J. Forniés, B. Gil, J. Gómez, E. Lalinde and M. T. Moreno, *Organometallics*, 2006, **25**, 2274–2283.
11 Additional issues associated with the refinements and structure solutions are treated at length in the ESI.† The large thermal ellipsoid of the nitrogen atom in **2**·Hb^+I^-3.75$CHCl_3$·2.83C_7H_8 (middle, Fig. 1) strongly suggests unresolved disorder. The morpholine nitrogen atom in **1**·Hc^+Cl^- is assigned to the position that gives the shortest NH···C_{sp} distances. To better represent the quality of the data, hydrogen bond lengths are only given to the hundredth of an Ångstrom.
12 Such substitutions can be promoted by transition metals. See for example: T.-S. Peng, C. H. Winter and J. A. Gladysz, *Inorg. Chem.*, 1994, **33**, 2534–2542.
13 L. N. Kuleshova and P. M. Zorkii, *Acta Crystallogr., Sect. B: Struct. Crystallogr. Cryst. Chem.*, 1981, **37**, 1363–1366.
14 S. Shirakawa, Quaternary Ammonium, Phosphonium, and Tertiary Sulfonium Salts as Hydrogen-Bonding Catalysts, in *Anion-Binding Catalysts*, ed. O. Garcia Mancheño, Wiley-VCH, Weinheim, 2022, ch. 8.
15 Prof. T. Lis (University of Wroclaw), exploratory experiments.
16 K. Nakanishi, T. Goto and M. Ohashi, *Bull. Chem. Soc. Jpn.*, 1957, **30**, 403–408.
17 (*a*) For a detailed review, see: G. Pagès, V. Gilard, R. Martino and M. Malet-Martino, *Analyst*, 2017, **142**, 3771–3796; (*b*) For applications focused on inorganic and organometallic chemistry, see: P. S. Pregosin, P. G. A. Kumar and I. Fernández, *New Chem. Rev.*, 2005, **105**, 2977–2998.
18 E. S. Stoyanov, I. V. Stoyanova and C. A. Reed, *Chem. – Eur. J.*, 2008, **14**, 7880–7891.
19 (*a*) T. Steiner, M. Tamm, A. Grzegorzewski, N. Schulte, N. Veldman, A. M. M. Schreurs, J. A. Kanters, J. Kroon, J. van der Maas and B. Lutz, *J. Chem. Soc., Perkin Trans.*, 1996, **2**, 2441–2446; (*b*) J. M. A. Robinson, B. M. Kariuki, R. J. Gough, K. D. M. Harris and D. Philip, *J. Solid State Chem.*, 1997, **134**, 203–206; (*c*) W. Guo, E. Galoppini, R. Gilardi, G. I. Rydja and Y.-H. Chen, *Cryst. Growth Des.*, 2001, **1**, 231–237; (*d*) M. S. Khan, M. R. A. Al-Mandhary, M. K. Al-Suti, T. C. Corcoran, Y. Al-Mahrooqi, J. P. Attfield, N. Feeder, W. I. F. David, K. Shankland, R. H. Friend, A. Köhler, E. A. Marseglia, E. Tedesco, C. C. Tang, P. R. Raithby, J. C. Collings, K. P. Roscoe, A. S. Batsanov, L. M. Stimson and T. B. Marder, *New J. Chem.*, 2003, **27**, 140–149; (*e*) T. S. Thakur, R. Sathishkumar,

A. G. Dikundwar, T. N. G. Row and G. R. Desiraju, *Cryst. Growth Des.*, 2010, **10**, 4246–4249; (*f*) J. D. White, L. E. Guzman, L. N. Zakharov, M. M. Haley and V. J. DeRose, *Angew. Chem., Int. Ed.*, 2015, **54**, 1032–1035.

20 T. E. Müller, S. W.-K. Choi, D. M. Mingos, D. Murphey, D. J. Williams and V. W.-W. Yam, *J. Organomet. Chem.*, 1994, **484**, 209–224.

21 (*a*) D. M. Dougherty, *Acc. Chem. Res.*, 2013, **46**, 885–893; (*b*) A. S. Mahadevi and G. N. Sastry, *Chem. Rev.*, 2013, **113**, 2100–2138.

22 A. Haque, R. A. Al-Balushi, I. J. Al-Busaidi, M. S. Khan and P. R. Raithby, *Chem. Rev.*, 2018, **118**, 8474–8597.

23 J. Koller, J. Grdadolnik and D. Hadži, *J. Mol. Struct.: THEOCHEM*, 1992, **259**, 199–209.